



Improved Analytical Solution for Water Hammer in Viscoelastic Pipes

Hossam A.A. Abdel-Gawad*

KEYWORDS:

Water hammer
Viscoelastic pipes
Maximum pressure
Analytical solution

Abstract— The challenge of the present paper is improving an analytical solution for the one-dimensional water hammer in viscoelastic pipeline due to sudden end valve closure. The importance of the analytical solution is providing the necessary design information, especially in absence of an analyzing software. New exact dimensionless analytical equation is derived to determine the attenuated pressure wave head along the first pressure wave trip, and the viscoelastic term is merged in the wave celerity expression. Then, the integration process is utilized to rederive an approximate analytical equation for the pressure head at the valve during the first half pressure wave cycle, which involves the maximum design pressure head. Performance of the analytical results is compared with numerical results of the method of characteristics, for nearly all literature studies of the problem. Perfect performance for the analytical results is obtained for frictionless pipes that are a little bit distorted as the ratio, of the steady state friction head losses in the pipe to the Joukowsky pressure head, increases. Therefore, a nonlinear deterministic optimization algorithm is adopted to improve the integration constant of the friction term, which enhances the accuracy of the analytical results.

I. INTRODUCTION

The excessive use of viscoelastic pipes in water supply and irrigation systems draw the attention for studying their viscoelastic behaviors under transient flow conditions. This is an essential requirement for managing accurately various water resources systems under actual properties. The present paper is concerned only with analyzing analytically the one-dimensional water hammer problem in viscoelastic pipe due to sudden closure of downstream valve in a simple pipe system consisting of a tank-pipe-valve.

Due to the difficulty associated with the exact analytical solution of the one-dimensional governing equations of the transient flow problems because of the inherited nonlinearity, numerical solution is generally used to analyze the problem. In

case of elastic pipes, several numerical methods are used, as mentioned in [1,2]. However, limited efforts are developed to analyze viscoelastic pipes, e.g., the method of characteristics (MOC) [3], the finite volume method (FVM) [4] and recently the wave characteristic method (WCM) [2]. For the same computational effort, the MOC, which is the most popular numerical method used by the researchers, has a higher degree of accuracy of the calculated results with respect to the FVM, and almost has comparable accuracy according to the WCM [2].

To the author's knowledge, all the numerical programs used to analyze the present problem, were generated to handle a prespecified research problems and are not available to the designers. The necessity of the analytical solution not only stems from the accurate results of the analytical approach compared to the numerical one, but also due to lacking a commercial software to handle the problem.

Received: (11 June, 2022) - Accepted: (02 August, 2022)

*Corresponding Author: Hossam A.A. Abdel-Gawad, Houston, Irrigation & Hydraulics Department, Faculty of Engineering, Mansoura University, El-

Mansoura 35516, Egypt. Email: (hossamaaa@mans.edu.eg ; hossamgawad@yahoo.com).

Pipelines are usually designed under maximum pressure head resulting from sudden shutdowns of pumps or valves. Such pressure occurs within the first half wave cycle, with exception to the very long cross country elastic pipes which reach their pressure peaks in longer periods [5]. The subsequent two subsections are concerned with the analytical philosophy that can be used to analyze the proposed problem. Two analytical approaches are used to solve the present problem analytically.

A. First Analytical Approach

First approach is often started with manipulating the governing water hammer differential partial equations with the MOC. The produced two ordinary differential equations are handled to capture two analytical equations, i.e.: 1) the attenuated pressure head wave at the wave front during the first trip to the tank, and 2) the pressure head variation at the valve within the first half pressure wave cycle. The Joukowsky equation is used to substitute the change in the pressure head at the wave front with the change in the velocity or vice versa, and an integration process is used to conclude the pressure head at the valve.

For elastic pipes, two exact analytical equations were concluded to calculate the attenuated pressure head [6]. Exponential equation is derived for weak jumps, and hyperbolic equation for large jumps with adverse flow direction. Another approximate analytical equation was developed for pressure head at the valve [7]. The quasi-invariant principle along the characteristic lines was adopted, where the quadratic equation in the velocity behind the wave front was relaxed to a linear one.

Using an explicit expression for the head at the wave front, Liou [5] derived an exact exponential equation representing the attenuated pressure at the wave front in elastic pipe, and another approximate analytical equation for the pressure head at the valve. The same attenuated pressure equation with different process was concluded, [8], by differentiating the momentum and the continuity equations with respect to time and space, respectively, and eliminating the mixed derivatives to conclude a nonlinear wave equation in one dependent variable, i.e. second order differential equation in the flow velocity. Then, with assistance of the Taylor series, a simple approximate expression was derived for both head at the valve and velocity along the pipe length only within the first wave trip.

To the author's knowledge, Keramat and Haghghi [9] developed the only approximate analytical equation used for viscoelastic pipes using the present approach. Their work is dependent on the unknown velocities behind the propagated wave front and merged the retarded strain within the wave celerity. Thus, another technique is required to determine these unknown velocities to use that analytical equation. The present research is concerned with improving the work of Keramat and Haghghi [9] to be easily applicable, by determining analytically the exact analytical velocity at the pressure wave front and rederiving an approximate analytical equation for the pressure head at the valve during the first half pressure wave cycle.

Jones and Wood [10] developed an analytical solution for gradual closure of the valve by lumping the effect of quadratic friction loss at one or several imaginary orifices along the elastic pipe. That study is applicable only under the assumption of non-reversal flow within the pipe, i.e. partial closing of the valve. Recently, an approximate analytical method was derived [11] for the accumulated pressure head at the valve, during the first half pressure wave cycle. This method considers, only, frictionless elastic pipes consisting of two reaches with lower hydraulic impedance for the reach associated to the valve.

B. Second Analytical Approach

The second approach is based on decomposing the mathematical representation, i.e., both the governing equations and the boundary conditions, into multiple solvable problems, and with the superposition principle the final solution can be achieved. Han et al. [12] used the multiple scales asymptotic analysis method that is based on recognizing the effective time scales of the different parts of the governing equations, and representing each time scale by additional independent times variables. The dependent variables, flow velocity and pressure head, are expanded along both original and additional time scales and by equating the produced terms at every time scale, several differential equations are separated and solved analytically in consecutive steps. The longest time scale limits the validity range of the solution, while increasing the number of terms adopted from the expansion series enhances its accuracy. That method was employed to describe an approximate analytical solution for an inclined elastic pipe due to sudden valve closure [13]. Later, it was applied for blood hammer within nonuniform artery radius and laminar flow condition [14], and for water hammer in medium viscoelastic pipe with only one weak feedback Kelvin element [15]. While the method can simulate the whole pressure wave pattern for the longest time scale, it hasn't a closed form for the analytical expressions that represent the water hammer in any viscoelastic pipe. Depending on the varied range of the retarded times and modulus of elasticity for different Kelvin elements, various time scales and consequently analytical expressions can be produced.

Sobey [16,17] produced analytical infinite converging series to the linearized wave equation, i.e. second order nonlinear wave equation, extracted from cross differentiating of the original hyperbolic governing equations and neglecting one of the dependent variables. The non-homogeneity embedded, in both linearized wave equation and its boundary conditions, was treated by arranging the problem into two solvable ones and with assistance of the superposition principle, the final analytical solution was combined.

The different analytical solutions discussed in the present subsection cannot be solved easily, a complicated computations must be accomplished before catching the analytical results. Also, they have a limited degree of accuracy, due to the truncated error produced from using a limited number of terms from the infinite series that represent the exact analytical solutions. The multiple scale approach is dependent on retarded times of the Kelvin elements used to represent the viscoelastic properties of the pipe; consequently, the multiple time scales

analytical approach must be rederived for different pipes characteristics.

C. Objective and Layout of the Work

Due to absence of commercial software, the recent traditional analyses of transient flow in viscoelastic pipes are based on an improper simplification. That is ignoring the viscoelastic characteristics of the pipes and considering them as elastic pipes with a consequent significant overestimation for the calculated pressure heads and capital costs of the pipes. Until now, there are no straightforward easy and applicable analytical equations that can be used to solve the present problem by a hand calculator or an Excel spreadsheet. The proposed analytical solution tackles that disadvantage.

The remaining of the present paper consists of three sections. Section II is concerned with the governing equations and the proposed analysis of both the exact attenuated pressure head at the front of the first propagated wave, and the approximate analytical pressure head at the valve during the first half pressure cycle. Different results are presented, compared with the MOC results, and discussed in subsections III.A and III.B. Subsection III.C is concerned with improving integration accuracy by updating the friction term using a deterministic nonlinear optimization approach. Finally, conclusions and recommendations are presented in section IV.

II. METHODOLOGY

A. Governing Equations

Simplified continuity and momentum equations, used to simulate the one dimensional transient flow in viscoelastic pipes, are [9,18]:

$$\frac{\partial H}{\partial t} + \frac{a^2}{g} \frac{\partial v}{\partial x} + \frac{2a^2}{g} \frac{\partial \varepsilon_r}{\partial t} = 0 \tag{1}$$

$$g \frac{\partial H}{\partial x} + \frac{\partial v}{\partial t} + \frac{fV|V|}{2D} = 0 \tag{2}$$

where:

$$\varepsilon_r(t) = J(s) * d\sigma'(t - s) = \sigma'(s) * dJ(t - s), \tag{3}$$

$$J(s) = \sum_{i=1}^{N_k} J_i(s) = \sum_{i=1}^{N_k} J_i \cdot \left(1 - \exp^{-\frac{s}{\tau_i}}\right), \tag{4}$$

$$\begin{aligned} \therefore \varepsilon_r(t) &= \sum_{i=1}^{i=N_k} \varepsilon_{ri}(t) \\ &= z \cdot \sum_{i=1}^{i=N_k} \left| \int_{s=0}^{s=t} \frac{\partial H'(t-s)}{\partial s} J_i \cdot \left(1 - \exp^{-\frac{s}{\tau_i}}\right) ds \right| \\ &= z \cdot \sum_{i=1}^{i=N_k} \left| \int_{s=0}^{s=t} H'(s) \cdot \frac{J_i}{\tau_i} \cdot \exp^{-\frac{(t-s)}{\tau_i}} ds \right|, \end{aligned} \tag{5}$$

H is the hydraulic head measured from a horizontal datum passing the valve center line, t is elapsed time from the onset of the transient action, a is constant wave celerity, g is gravity acceleration, V is average liquid velocity within the pipe cross section, x is distance along the pipe measured from the tank, see Fig. 1, D is inner pipe diameter, f is Darcy friction factor, ε_r is retarded strain within the viscoelastic pipe, $*$ is Sieltjes convolution operator, ε_{ri} is the retarded strain of Kelvin element i , N_k is number of Kelvin elements, $z = \alpha \rho g D / (2e)$ is a constant,

$\sigma' = z \cdot H'$ is the change in pipe wall internal stresses, α is a pipe fixation factor, ρ is liquid density, e is pipe thickness, H' is the net change in the pressure head = $H - H_0$, H_0 is the initial steady hydraulic head, $J_i(s)$ is the creep compliance function for Kelvin element i at time s , $J_i = J_i(\infty) = 1/E_i$ is the creep compliance coefficient for Kelvin element i , and E_i , τ_i are modulus of spring elasticity and retardation time for Kelvin element i , respectively.

Minor terms with insignificant effect $V \partial H / \partial x$ and $V \sin \theta$ are eliminated from (1), where θ is the pipe slope, which is positive upward, and minor term $V \partial V / \partial x$ is ignored in (2). Equations (1) and (2) can be transformed to a dimensionless form using (6):

$$X = \frac{x}{L}, v = \frac{V}{V_0}, T = \frac{t \cdot a}{L}, h = \frac{H}{\Delta H_0}, \Delta H_0 = \frac{a \cdot V_0}{g}, \varepsilon = \frac{\varepsilon_r}{\Delta H_0} \tag{6}$$

where X and T are the dimensionless independent variables that represent relative distance from the tank and relative time, respectively, h and v are dimensionless dependent unknown variables represent relative hydraulic head and relative velocity, respectively, L is the total pipe length, V_0 is initial steady velocity along the pipe, ΔH_0 is the Joukowski pressure head due to sudden valve closure. The dimensionless governing equations become:

$$\frac{\partial h}{\partial T} + \frac{\partial v}{\partial X} + \frac{2a^2}{g} \frac{\partial \varepsilon}{\partial T} = 0 \tag{7}$$

$$\frac{\partial h}{\partial X} + \frac{\partial v}{\partial T} + \frac{fLV_0}{2aD} v|v| = 0 \tag{8}$$

where,

$$\begin{aligned} \varepsilon(T) &= \frac{\varepsilon_r(t)}{\Delta H_0} = \frac{\sum_{i=1}^{i=N_k} \varepsilon_{ri}(t)}{\Delta H_0} \\ &= z \cdot \sum_{i=1}^{i=N_k} \left| \int_{s=0}^{s=T} \frac{\partial h'(T-s)}{\partial s} J_i (1 - \exp^{-s \cdot U_i}) ds \right| \\ &= z \cdot \sum_{i=1}^{i=N_k} \left| \int_{s=0}^{s=T} h'(s) \cdot \frac{U_i}{E_i} \cdot \exp^{-U_i(T-s)} ds \right|, \end{aligned} \tag{9}$$

ε represents the retarded strain, ε_r , as a function of the relative change in the hydraulic head $h' = H' / \Delta H_0$, instead of H' , and $U_i = L / (a \tau_i)$ is a dimensionless parameter that represents the ratio of the time required for the pressure wave to travel the total pipe length to the retardation time of the Kelvin element i .

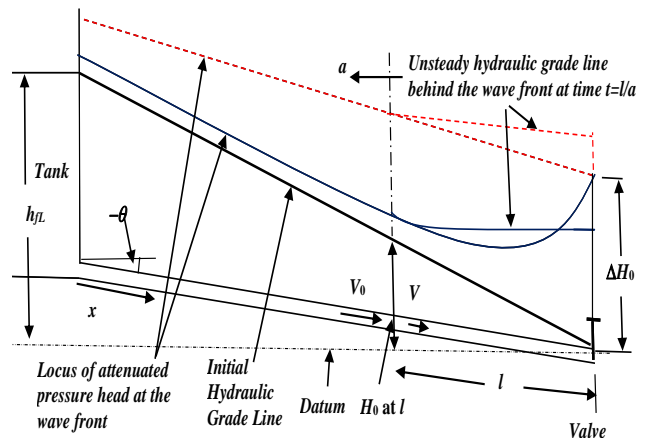


Fig. 1 Propagated pressure wave head ΔH over the initial hydraulic grade line for: 1) elastic pipe (dotted curve), 2) viscoelastic pipe (straight curve).

B. Attenuated Pressure Wave Head

As mentioned previously, in the introduction section, two analytical approaches are always used to find the analytical solutions. The first approach retains with direct solvable analytical equations, and it is succeeded in concluding direct applicable analytical equations for the elastic pipes only. Whereas the second one needs more complicated calculations, acceptance of a limited degree of accuracy, and some solutions must be rederived depending on the characteristics of the viscoelastic pipe. Therefore, the first approach is adopted here, which is based on integrating the ordinary differential equations generated from applying the MOC on the partial differential governing equations.

It is worth to mention that by ignoring both the retarded strain (i.e., elastic pipe) and the friction (i.e., frictionless pipe), from the governing equations (1) and (2) respectively, the MOC leads to exact analytical solution. For frictional pipe, the numerical values of the pressure wave heads or the velocities at the propagated wave front are an inevitable essential requirement for integrating the ordinary differential equations produced from the MOC. Thus, the task of the present section is to produce an exact analytical equation for the increase in the pressure head at the wave front or the flow velocity just behind that wave, for the first wave trip from the valve to the tank.

Sudden closure of the downstream valve, see Fig. 1, generates an instantaneous pressure wave head, ΔH_0 , at the valve, that is propagated upstream with celerity a , over the initial steady hydraulic grade line (HGL). For frictional elastic pipes, as the pressure wave travels upstream, it moves upward over the initial slope of the HGL. To satisfy the updated slope of the HGL, the celerity behind the wave front will not reduce to zero. Consequently, some flow crosses the wave front causing an accumulated liquid mass behind it, named line packing. As time elapses, the accumulated line packing produces a gradual time dependent rising in the HGL. In viscoelastic pipes, the viscous effect of the pipe wall will produce a retarded strain that enlarges the pipe cross section. Depending on degree of expansion, for the pipe cross section, the accumulated flow mass behind the wave front can be stored without excess in the pressure head downstream the wave front. However, in the case of a considerable high degree of viscoelasticity, the enlargement in the pipe volume is more than the accumulated mass, which produces pressure head drops.

The MOC is used here to estimate the pressure wave head, at the wave front, as it propagates along the pipe for $T \leq 1$. Instantaneous pressure wave head equals to $\Delta H = a(V_0 - V)/g$, and in a dimensionless form can be represented as $\Delta h = \Delta H/\Delta H_0 = 1 - v = -\Delta v$, where $\Delta v = (V - V_0)/V_0$ is the instantaneous relative drop in initial liquid velocity at the wave front. The ordinary differential equation along the first characteristic line C^- , see Fig. 2, can be determined by subtracting (7) and (8) and considering $\partial X/\partial T = (1/a)\partial x/\partial t = -1$, as:

$$\frac{dh}{dT} - \frac{dv}{dT} + Rv^2 + \frac{2a^2}{g} \frac{\partial \varepsilon}{\partial T} = 0 \quad (10)$$

where, $R = fLV_0/(2aD)$ is a dimensionless ratio of the total steady friction head loss along the pipe length $h_{fL} = fLV_0^2/(2gD)$, to the Joukowsky pressure head ΔH_0 . During the pressure wave first trip along the pipe, the velocity direction/sign is not varied and remains positive from the tank to the valve, thus $v|v|$ can be replaced by v^2 in (8). Applying the Leibniz rule for the derivative of (9) with respect to T , the last term in (10) can be represented as:

$$\frac{2a^2}{g} \frac{\partial \varepsilon}{\partial T} = -\frac{2a^2}{g} \sum_{i=1}^{N_k} U_i \varepsilon_i + \sum_{i=1}^{N_k} U_i \cdot Y_i \cdot h'(T) \quad (11)$$

where, $\varepsilon_i = \varepsilon_i/\Delta H_0$ is the Kelvin element strain as a function of h' instead of H' and instantaneously equal to zero at the wave front, and Y_i is a dimensionless parameter equal to $\alpha \rho D a^2 / (e \cdot E_i)$ for the Kelvin element i . Different terms of (10) are compensated as: the viscoelastic term is substituted from (11), dv/dT by $d\Delta v/dT = -d\Delta h/dT$, h by $[h_{fL} - fLV_0^2/(2gD) + \Delta H]/\Delta H_0$, dh/dT by $[R + d\Delta h/dT]$, and $(1 - v^2)$ by $(1 - v) \cdot (1 + v) = -\Delta v(2 + \Delta v) = \Delta h(2 - \Delta h)$. Then, (10) can be represented by a nonlinear ordinary differential equation as:

$$2 \frac{d\Delta h}{dT} + (2R + Z)\Delta h - R(\Delta h)^2 = 0 \quad (12)$$

where, $Z = \sum_{i=1}^{N_k} Z_i = \sum_{i=1}^{N_k} U_i \cdot Y_i = \frac{\alpha \rho D a L}{e} \cdot \sum_{i=1}^{N_k} \frac{J_i}{\tau_i}$. Solving (12) with the valve boundary condition, i.e. $\Delta h = 1$ at $T = 0$, the following exact analytical equation is obtained, [19]:

$$\Delta h = -\Delta v = \frac{2R + Z}{R + (R + Z) \exp^{(R + 0.5Z)T}}, \quad 0 \leq T \leq 1 \quad (13)$$

Neglecting the viscoelastic term, Z , leads to an analytical equation for elastic pipe [5,6,8]. Equation (13) shows the extra effect of viscoelasticity, Z , in attenuating the propagated pressure wave head. In contrast to the constant propagated pressure head in a frictionless elastic pipe, (ΔH_0 at $R = 0$), viscoelasticity adsorbs that pressure head with propagation. From (13), it is interesting to note that the relative behavior of the dimensionless dependent variables, h and v , at the propagated wave front will be the same for different combinations of flow and pipe characteristics that have the same R and Z .

C. Pressure Head at The Valve

Fortunately, the relative strain ε at the wave front is zero for $T \leq 1$, this enables a straightforward replacing of $d\varepsilon/dT$ with h' in (10). This is not the case when handling the ordinary differential equation along the characteristic line C^+ , see Fig. 2, as the unknown relative strain, ε , along that line must be known in advance. To handle that problem, the strain rate, $\partial \varepsilon_r / \partial t$ in (1), is inset within the constant wave celerity, a , during the first half pressure wave cycle, i.e. $T \leq 2$. Applying the Leibniz rule for the derivative of the second part of (3), with respect to t , and assuming a linear change in the pressure head H' with time, then [9]:

$$2 \frac{\partial \varepsilon_r}{\partial t} = 2z \cdot \frac{\partial}{\partial t} \int_0^t H'(t-s) \cdot \frac{dJ(s)}{ds} ds \cong 2z \cdot \frac{\partial H'}{\partial t} \cdot J(t) \quad (14)$$

where $\partial H'/\partial t = \partial H/\partial t$. From (1) and (14), the following continuity equation is obtained, [9]:

$$\left[\frac{\rho g}{k} + \frac{z}{E_0} + z \cdot J(t) \right] \frac{\partial H}{\partial t} + \frac{\partial V}{\partial x} = \frac{g}{c^2} \frac{\partial H}{\partial t} + \frac{\partial V}{\partial x} = 0 \quad (15)$$

where,

$$\frac{1}{c(t)} = \sqrt{\frac{\rho}{k} + \frac{\alpha \rho D}{e} \left[\frac{1}{E_0} + \sum_{i=0}^{N_k} \frac{1}{E_i} \left(1 - \exp \frac{-t}{\tau_i} \right) \right]}, \quad (16)$$

$c(t)$ is a time dependent wave celerity and equal to, a , at time = 0, k is the modulus of liquid elasticity, and $J_0 = 1/E_0$ is the inverse of instantaneous modulus of elasticity for the pipe wall.

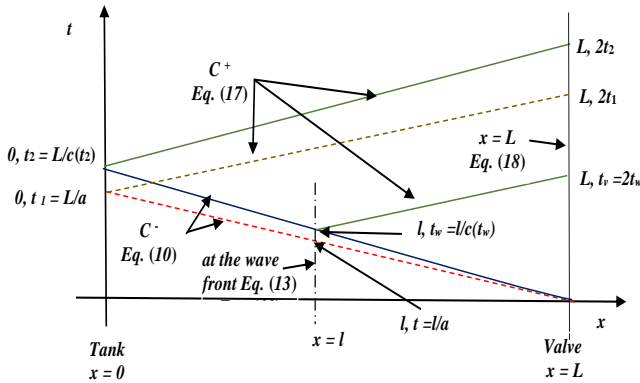


Fig. 2 Characteristic lines for constant wave speed a , the dashed lines; and characteristic curves for time dependent wave speed $c(t)$, the continuous curves. (The figure shows the application positions of the different equations)

Adding (2) and (15), and considering $\partial x/\partial t = c(t)$, the ordinary differential equation along the positive characteristic curve, C^+ , can be represented as, (17):

$$\frac{g}{c} \frac{dH}{dt} + \frac{dV}{dt} + \frac{fV|V|}{2D} = 0 \quad (17)$$

Integrating that ordinary differential equation (17) along the positive characteristic curve C^+ , between the wave front position at any point along the pipe and the valve, leads to a direct dimensional equation, (18a), for the unknown hydraulic head at the valve, that is valid for the first half pressure cycle. A dimensionless form of (18a) is presented in (18b):

$$H_v|_{2t} = \frac{c(t_v)}{c(t_w)} H_w|_{t_w} + \frac{c(t_v)}{g} V_w - \frac{f \cdot c(t_v)}{2gD} \int_{t_w}^{t_v} V^2 dt = \frac{c(t_v)}{c(t_w)} \left(\frac{f l_{wv} V_0^2}{2gD} + \Delta H_w \right) + \frac{c(t_v)}{g} (V_0 + \Delta V_w) - \frac{f l_{wv} V_w^2}{2gD P} \quad (18a)$$

then,

$$h_v(2T) = RTc(t_v)/c(t_w) + c(t_v)/a - RTv_w^2/P \quad (18b)$$

where,

$$0 \leq t \leq \frac{L}{a}, \quad 0 \leq t_w \leq \frac{L}{c(t_2)}, \quad t_v \approx 2t_w, \quad 0 \leq (T = l_{wv}/L) \leq 1$$

H_v and H_w are the pressure heads at the valve and the propagated wave front, respectively, t_w is the required time for

the wave front to travel the length l_{wv} along the pipe, V_w is the velocity just behind the wave front, $v_w = V_w/V_0$ is the relative velocity and can be determined from (13) by substituting $T = l_{wv}/L$, $\Delta V_w = V_w - V_0 = -g \cdot \Delta H_w/c(t_w)$ is the sudden drop in the velocity behind the wave front, ΔH_w is the sudden increase in the hydraulic head at the wave front, $h_v(2T) = H_v|_{2t}/\Delta H_0$ is the relative pressure head at the valve at the dimensionless time $2T$ which represents the real time $2t$ in the dimensionless form, and P is a coefficient that depends on the velocity distribution shape within the pipe along C^+ from the wave front at time t_w to the valve at time $t_v = 2t_w$, see Fig. 2. Assuming a linear change of the velocity from V_w to zero, as proved by Liou [5] for elastic pipes, leads P to be equal 3, see Appendix A. An improvement of that assumption is studied in the subsequent subsection III. C. It is worthy to notice that neglecting the viscosity effect and using constant wave celerity, in (18b), leads to the same dimensionless analytical equation derived by Liou [5] for elastic pipes.

Wave celerity c is decreased exponentially, with elapsed time, from the initial elastic wave celerity $a = c(0)$ to $c(\infty)$, thus as the wave is propagated, both $c(t_w)$ and $c(t_v)$ approach $c(\infty)$. The traveling length l_{wv} is considered equal to the elapsed time t_w multiplied by the final wave celerity $c(t_w)$, instead of the average of the variant celerity along the travel path, with insignificant error. Calculation of the average wave celerity along the pipe is restricted only to numerical integration of $c(t)$, see (16), which complicates the analytical process and increases the computation effort. The expected errors from adopting any assumption including replacing the average wave celerity along the pipe with the final one at the wave front, will be examined later in subsections III.B and III.C. Integration of the first term of (17) is presented in Appendix B.

While the proposed process, used for deriving the present analytical equations, is based on the soul of the previously published work by Keramat and Haghghi [9], there are noticeable differences in the final results due to the following points:

- 1) despite of using a decreasing celerity approach for the propagated wave seems more logical, all the current numerical methods, used to simulate transient flow in viscoelastic pipes (MOC, WCM, FVM), are based on using a fixed celerity approach to preserve a constant discretization mesh between subsequent transient time steps. The present analytical equations and the numerical methods lead to a difference in the elapsed time necessary for travelling the first half wave, equal to $2[L/c(t_2) - L/a]$ at the valve see Fig. 2, with consequent nonidentical extension for the first pressure wave half cycle. Therefore, other criteria unlike the elapsed time must be adopted to make the results of the two approaches comparable. The main energy source that creates the water hammer is the sudden drop of the velocity within a certain volume of the water, thus it is fair to compare the results at constant volumes affected, i.e. the same travelled lengths of the pipe by both the fixed celerity and the decreasing one. Thus, the analytical pressure head at the valve at time $2t_w = t_v$, must be compared with the numerical one at time equal to $2t = 2l_{wv}/a = 2t_w \cdot c(t_w)/a$, as done in the left-hand side of (18a).

- 2) the first term in the right-hand side in (18 a) and (18 b) is multiplied by $c(t_v)/c(t_w)$, instead of one [9], which is produced from the integration process. That factor of multiplication has a variant range with an initial value 1 to about 0.9 in the early time steps, depending on the pipe characteristics, then it increases again with elapsed time to approach 1. It is found that this factor gives a more accurate results with respect to fine MOC results in cases of studying short pipes or at early time steps for any pipe length. The period which is affected by that factor can be estimated as $3\tau_{max}$, i.e. when all the exponents in the last term in (16) approach zeros.
- 3) A clear form for the friction's contribution is found in the last term in (18a), which is based on the present concluded exact velocity behind the wave front, (13). Consequently, the proposed analytical equations (18 a) and (18 b) have no need to adopt a special technique to evaluate the friction term in advance as its requested by Keramat and Haghghi [9].

D. Steps of The Analytical Solution

The required steps to exploit the proposed analytical solution, for the pressure head at the valve, can be summarized as follows:

- 1) determine the wave celerities $a = c(0)$, and $c(\infty)$ from (16),
- 2) calculate the dimensionless variables $R = fLV_0/(2aD)$, and $Z = \frac{\alpha \rho D a L}{e} \cdot \sum_{i=1}^{N_k} \frac{J_i}{\tau_i}$,
- 3) estimate the required time for the wave to travel from the valve to the tank, t_2 , which can be initially assumed as $t_2 = L/c(\infty)$, then by using (16) repeatedly by trial and error, t_2 is adjusted and decreased to $L/c(t_2)$,
- 4) for any chosen time, $0 < t_w < t_2$, calculate both $c(t_w)$ and $c(t_v = 2t_w)$ using (16),
- 5) the dimensionless time corresponding to t_w is $T = c(t_w) \cdot t_w / L = l_{ww}/L$,
- 6) the relative velocity just behind the wave front, $v_w = V_w/V_0$, can be calculated from (13) using T , and
- 7) Finally, determine the unknown pressure head, H_v , at the valve at time $t_v = 2 t_w$, from (18a), or its dimensionless form, h_v at the dimensionless time $2T$, from (18b).

For the rest of the research, the dimensionless form of the pressure head, i.e., (18b), is used to facilitate the comparison between different results, as they are scaled to the dimensionless relative variables T and h .

III. RESULTS AND DISCUSSION

TABLE (1)
LITERATURE DATA OF FLOW AND VISCOELASTIC PIPES CHARACTERISTICS

Plastic types	Ref.	L m	f	D mm	e mm	V ₀ m/s	J ₀ (10 ⁻¹⁰ pa ⁻¹)	J _i (10 ⁻¹⁰ Pa ⁻¹)	T _i s	Y _∞ ΔJ/J ₀	R	Z
HDPE	[3,20]	277	0.0252	50.6	6.3	0.54*	7.0	1.057, 1.054, 0.9051, 0.2617, 0.7456	0.05, 0.5, 1.5, 5, 10	0.575	0.094	2.4
	[21]	103.2	0.01823	44	3	2.05	8.302	2.17, 1.7, 0.91	0.03, 0.5, 3	0.6	0.149	3.3
	[22]	554	0.02	50.6	6.3	0.15*	6.92*	1.044, 1.037, 1.145	0.05, 0.5, 1.5	0.46	0.04	4.7
	[23]	138.8	0.0182	44	3	2.36	5.4	0.645, 0.415, 0.96, 0.263, 0.453	0.05, 0.5, 1.5, 5, 10	0.507	0.19	1.1
	[24]	220	0.0205*	93.3	8.1	0.63*	6.3	0.6, 1.052, 1.12	0.08302, 0.6538, 40.35	0.44	0.038	0.8
MDPES	[25]	37.2	0.035*	22	1.6	0.3	15.5	7.54, 10.46, 12.37	0.000089, 0.0222, 1.864	1.96	0.042	960
LDPE	[26,27]	43.1	0.024*	41.6	4.2	0.57	17.9 ^a	10.09, 13.97, 16.28	0.000115, 0.0221, 1.822	2.25	0.03	891
PVC	[28]	203.2	0.024*	75	5.2	0.4*	3.258	0.225	0.05	0.07	0.028	0.6
	[29]	275.2	0.023*	235.4	7.3	0.16	3.44	0.0848, 0.1136	0.05, 0.5	0.058	0.006	0.4

* calculated from the available reference data.
^a at temperature 31 °C

Previous literature is reviewed to specify the logical range of variations in the three dimensionless parameters U , Y , and Z . Four different plastic materials are found in the literature as: 1) High density polyethylene (HDPE), 2) Medium density polyethylene (MDPE), 3) Low density polyethylene (LDPE), and 4) Polyvinyl chloride (PVC), see Table 1.

The first dimensional parameter, $U = \sum U_i$, is mainly dependent on the total pipe length and the retarded times of different Kelvin elements. In general, the retarded times of Kelvin elements are taken as $0.0 s < t < 10 s$, Table 1, with

exception of one HDPE case, that has a retarded time for a Kelvin element equal to 40.35 s. From the data in Table 1, the magnitude of U reaches an upper value of 37.2 for both HDPE and PVC pipes and inflated to more than 1500 for both MDPE and LDPE pipes. However, U increases for all pipe materials with increasing the pipe length.

The dimensionless parameter, $\sum Y_i$, is dependent on a^2 and $\sum J_i$. The compressibility effect of water that is represented by the term ρ/k , (16), is nearly about $4.65 \times 10^{-7} s^2/m^2$. For $\alpha = 1$ and with a lower practical ratio of $D/e = 8$, the elastic

contribution of the pipe wall, $\alpha\rho DJ_0/e$, is within the range $2.6 \times 10^{-6} - 1.19 \times 10^{-5} \text{ s}^2/\text{m}^2$ which is larger than ρ/k by 5.6 to 25 times. Therefore, the effect of water compressibility can be skipped, without significant error, to achieve a simple representation for the dimensional parameter Y as, the ratio of the summation of the creep coefficients for different Kelvin elements to the reciprocal of instantaneous modulus of elasticity, $\Sigma J_i/J_0$, see Table 1. Thus, Y represents the degree of viscoelasticity of the pipe material and has a magnitude ≤ 0.6 for HDPE and PVC and increases to about 2 for MDPE and LDPE pipe. Accordingly, the dimensionless term Z can be simplified as $(L/a).\Sigma (J_i / J_0 \tau_i)$, with upper limits equal to 6.4 and 1 for HDPE and PVC pipes, respectively, while it increases to hundreds for both MDPE and LDPE due to the very small retarded time associated with the first Kelvin element, used to represent their viscoelastic behaviours. An essential requirement to obtain accurate results from the MOC is to discretize the time to steps with maximum magnitude $\leq \tau_{min}/2$, [18]. Thus, an expensive high number of nodes must be used to discretize both the MDPE and the LDPE pipes.

The PVC has the minimum level of viscoelasticity within the studied four plastic types, while the LDPE has the maximum. Ratio of the steady friction head to the Joukowsky pressure head, R , is between 0.006 and 0.22, and velocities are varied between 0.15 to 2.36 m/s.

A. Pressure Head at The Wave Front

The attenuation of the instantaneous dimensionless pressure head Δh , (13), at the propagated wave front is shown in Fig. 3 for $R = 0.005, 0.05, 0.1, 0.5, 1$ and $Z = 0.5, 5, 1, 5, 10, 100, 1000$. The y-axis represents the change in ΔH which is equivalent to $-\Delta v = 1-v$, while the x-axis represents the dimensionless time T from the moment of the sudden closure of the valve or the ratio of the travelled distance to the total pipe length X .

All propagated pressure waves are started with the Joukowsky pressure head, which is equal to 1 in the dimensionless form and decreases linearly, for $Z \leq 1$ with an increasing rate as R increases from 0.005 to 1. As Z becomes greater than 1, an exponential decrease with a decreasing rate, in ΔH , can be observed with a diminishing effect for variation of R , that becomes null for $Z \geq 100$. For $Z \geq 10$, the pressure wave head is completely absorbed within the pipe length due to the high viscoelasticity of the pipe wall.

Existence of exact analytical solution provides an excellent opportunity for measuring accuracy of the numerical methods. This gives an idea about the degree of reliability for the numerical methods when assessing the validity of the approximate analytical solution derived to predict the pressure head at the valve, i.e. (18 a) and (18 b).

The MOC, the most popular numerical method, is used here for analysing the water hammer problem and its results are compared with the exact analytical equation from (13). Figure 4 shows the logarithmic changes in errors in the results of the MOC with increasing the number of discontinuities/nodes (N_D) used to discretize the pipe. Two cases are studied for the HDPE and MDPE pipes as referenced in [22, 25], see Table 1. Two measuring error criteria which are the relative root mean square

error (RRMSE) and the relative absolute maximum error (RAMAX), are used:

$$RRMSE = \frac{1}{G_0} \sqrt{\frac{\sum_{m=1}^{N_D} (G_{c,m} - G_{ea,m})^2}{N_D}} \tag{19}$$

$$RAMAX = \frac{\text{Max.} \sum_{m=1}^{N_D} |G_{c,m} - G_{ea,m}|}{G_0} \tag{20}$$

where, G represents the dependent variable H or V at the propagated wave front as it marches along the pipe for the first trip, and the subscripts c, ea, m , and 0 mean calculated, exact analytical, discontinuity number, and initial magnitude of the variable, respectively. Numerous numbers of criteria can be adopted to measure the error between the MOC results and the corresponding analytical ones. The RRMSE is a good criterion to measure the relative average deviation for the MOC results from the analytical ones; as the RRMSE decreases to zero, both results go to be identical. On the other hand, the RAMAX criterion that measures the relative maximum absolute error, provides the designer with a reasonable data for estimating the factor of safety of the pipe.

According to Fig. 4, increasing N_D from 50 to 5000 improves the results of the HDPE case significantly with a recession in the measured error from 10% to 0.1%.

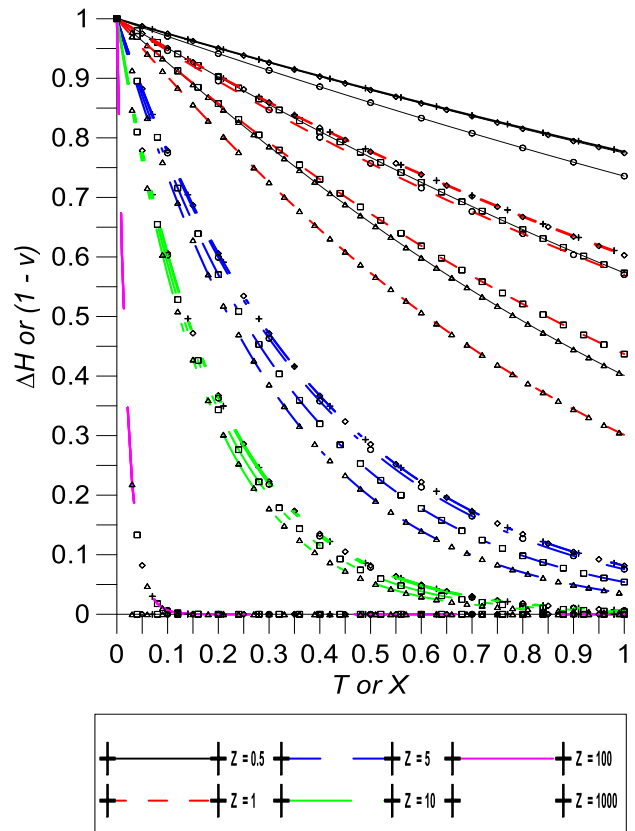


Fig. 3 Dimensionless increase in the pressure head at the wave front during propagation from the valve to the tank for different values of Z (represented by lines) and R (represented by symbols, $R = 0.005 +, 0.01 \diamond, 0.1 \circ, 0.5 \square, 1 \square$)

On the other hand, for the case of the MDPE even for dense pipe discretization with N_D equal to 5000, a significant error can be noticed with a 1% for RRMSE and 10% for RAMAX. This behaviour is expected due to the very small retardation time associated with the first Kelvin element which causes a

noticeable error/oscillation at earlier time intervals. If the distorted results of the first few time steps are eliminated, the maximum RAMAX will be located at the last time step with a magnitude of the same order of the RRMSE, as shown in Table 2.

The parameter Z decreases from 960 (MDPE, [25]) to 4.7 (HDPE, [22]), with a logarithmic decrease in the magnitudes of the two measuring error criteria, see Fig. 4. As the viscoelastic characteristics of the pipe changed to PVC, the parameter Z decreases to 0.6, see Table 1, with negligible measuring errors for the two criteria.

For the two previous cases, unexpectedly, an unequal relative degree of error is observed for the velocity and the pressure head. More accurate results can be achieved by the MOC for the pressure head at the wave front than the results of the velocity behind the wave. This behavior is due to the simplification assumptions suggested to represent both the friction and the retarded strain rate terms within the numerical skeleton for the MOC.

B. Pressure Head at The Valve

To check the effect of different assumptions, adopted to derive the proposed analytical equation for the pressure head at the valve, all literature cases presented in Table 1 are solved analytically with (18b) and numerically by the MOC. A relative fine discretization of the pipe is considered with ND equal to 5000. The two error criteria, (19) and (20), are considered to measure the degree of accuracy for the analytical solution, Table 2.

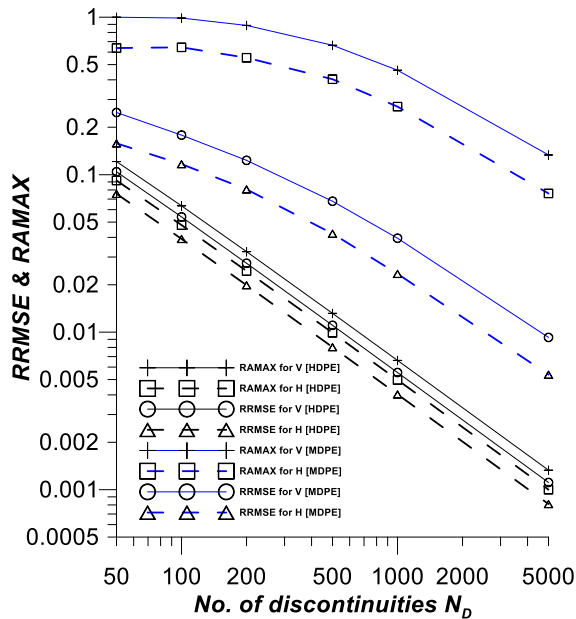


Fig. 4 Effect of increasing N_D against two measuring error criteria (RRMSE and RAMAX) for two cases (HDPE and MDPE).

For the four material types, the maximum RRMSE are varied between 1.09% and 0.00372%. On the other hand, the maximum RAMAX are located at the last time steps with 2.04% for HDPE and 0.02% for PVC, while the RAMAX appears at the first time step for MDPE and LDPE pipes with a maximum value equal to 6.16% and decreases rapidly within the first few elapsed time steps to approach zero, then it starts

to increase again with time to another maximum value, at the last time step, equal to 0.998%. Deceptive behaviors of the MOC for both MDPE and LDPE pipes at the initial time steps are expected; therefore, the maximum RAMAX can be considered as 0.998%.

Three different cases are selected as presented in Table 2, which are associated with the worst degree of error, to investigate the pressure head at the valve using both the MOC and the proposed analytical equation. Both MDPE and LDPE pipes have nearly similar properties and are represented with one case [26,27]. These cases are considered under three conditions: 1) effect of both friction and viscoelasticity ($R \neq 0, Z \neq 0$), 2) effect of friction only ($R \neq 0, Z = 0$), and 3) effect of viscoelasticity only ($R = 0, Z \neq 0$). The analytical equation presented by Keramat and Haghighi [9] cannot be applied to frictional pipes without adopting a method to estimate the friction term in advance, thus the results of their analytical equation are presented in Figs. 5, 6, and 7 for comparison in case of frictionless pipes only.

TABLE (2) RELATIVE ERRORS BETWEEN THE ANALYTICAL SOLUTION AND THE MOC FOR THE PRESSURE HEAD AT THE VALVE.

Plastic types	Ref.	a m/s	ND _{min}	RAMAX x 10 ²	RRMSE x 10 ²
HDPE	[3,20]	393	30	1.11	0.489
	[21] ^s	286	25	2.04	1.09
	[22]	393	58	0.857	0.441
	[23]	345	18	0.832	0.311
	[24]	360	15	0.0652	0.0302
MDPEs	[25]	232	3605	5.97* 0.947	0.65
LDPE	[26,27] ^s	234.6	3197	6.16* 0.998	0.692
PVC	[28] ^s	440	20	0.0203	0.00916
	[29]	339	34	0.00928	0.00372

* max. error is occurred at the first time step.

^s selected cases for further analysis.

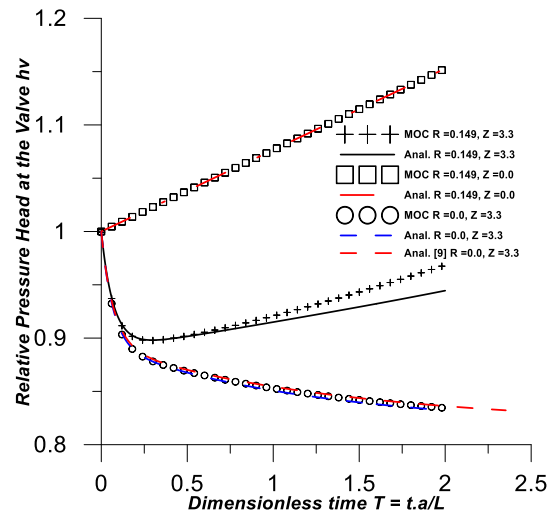


Fig. 5 Effect of friction, viscoelasticity, and both on the relative pressure head at the valve for the HDPE case [21].

Figures 5, 6, and 7 show the change in the relative pressure head, h_v , at the valve for both the analytical solution, (18b), and the MOC results with N_D equal to 5000. From the figures, several points can be observed as will be discussed below.

The analytical solution simulates the pressure head at the valve in a good way with a limited decrease in the solution accuracy as the dimensionless time T elapses from 0 to 2. This deterioration in accuracy is due to the assumption of the linear decrease for the velocity along the characteristic path C^+ from the wave front to the valve. Maximum RAMAX of h_v , for all the studied cases, is equal to 2.04% that can be accepted, whereas it is in the same range for the accuracy of the MOC results using a number of discontinuities equal to 200, Fig. 4.

For the three studied cases, under the effect of either friction or viscoelasticity only, the pressure head at the valve is the same for both the analytical and the MOC results with a very limited divergence in the case of LDPE, (Fig. 6). Ignoring the viscoelastic effect and considering only the instantaneous elasticity, will overestimate h_v significantly due to the accumulated backfill within the pipe with time.

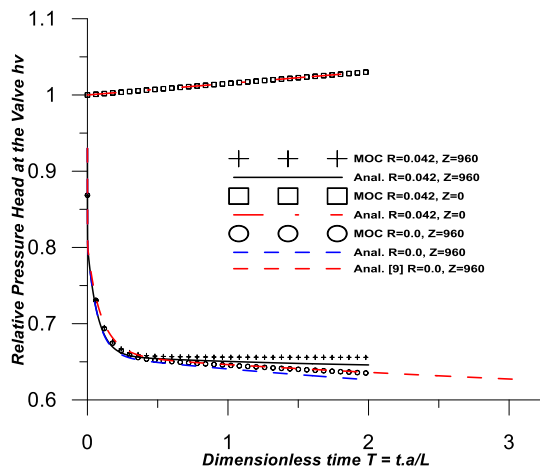


Fig. 6 Effect of friction, viscoelasticity, and both on the relative pressure head at the valve for the LDPE case [26,27].

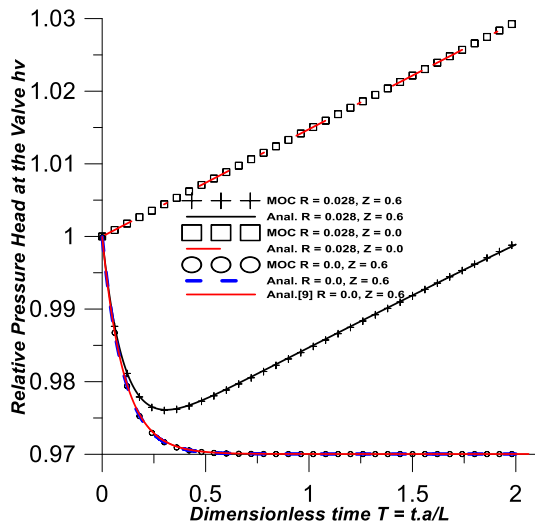


Fig. 7 Effect of friction, viscoelasticity, and both on the relative pressure head at the valve for the PVC case [28]

In the case of eliminating the friction effect, the pressure head at the valve, h_v , will continuously decrease with an exponential rate to a constant head depending on the dimensionless term Y . For the three cases, the effect of

viscoelasticity in reducing h_v , initially dominates the pressure excess due to the backfill. That dominance is waning as U increases or Y decreases. The analytical results produced by using Keramat and Haghighi analytical equation, [9], has very good matching with accurate MOC results, but with a longer dimensionless extension times for the first half period of the waves which are equal to 2.35, 3.122, 2.06, for the three cases studied, HDPE [21], LDPE [26,-27], and PVC [28] respectively. On the other hand, the exact dimensionless period produced using any available numerical method are 2.

C. Analysis of The Frictional Integration Variable P

Velocity distributions of flow along the positive characteristic line, C^+ , from the tank at $T = 1$ to the valve at $T = 2$, are shown in Fig. 8 for the three cases selected from Table 2. Two different pipe lengths for each case are considered as follows: 1) first length, equal to L , as mentioned in Table 1, and 2) second length equal to $10L$. As shown in Fig. 8, the irregular change between the different distributions is clearly noticed. This is contradictory between those irregular changes and the linearity assumption for the change in the velocity, as considered in subsection II.C, is the main cause of the error in the analytical solution. Therefore, the coefficient P must be adapted to assure that the last term in (18 a) and (18 b) represents accurately the accumulated friction losses along C^+ from the wave front to the valve. To achieve that goal, P is represented by a function of the different variables within the problem. A nonlinear deterministic optimization method, the Generalized Reduced Gradient (GRG) algorithm, is used to represent P as a function of these variables, by minimizing the RAMAX errors between the results of both the MOC and the analytical equation, (18a).

$$Obj_{min} = Max. \sum_{i=1}^{N_i} \sum_{j=1}^{N_j} \frac{|\Delta H_{v_{i,j}} + FRIC_{i,j} / P((D/e, J_0, J/J_0, \tau, R)_i, T_{i,j})|}{\Delta H_{0,i}} \quad (21)$$

where, Obj_{min} means the objective function that must be minimized, $\Delta H_{v_{i,j}}$ is the difference between the MOC pressure head results at the valve for run i after elapsed time steps j , and the corresponding summation of the first two terms on the right hand side of (18 a), $FRIC_{i,j}$ represents the last term in (18a), $P()$ is the suggested function, $\Delta H_{0,i}$ is the Joukowski pressure head for run i , N_i is the number of executed runs or combinations of data used to generate the necessary data essential to calibrate the P function, and N_j is the number of time steps at which the output data are collected. The GRG algorithm is selected due to the following advantages: 1) limited computational effort with respect to any stochastic optimization methods, 2) can handle any nonlinear problem, 3) it is free and available in the package “Solver”, which is a Microsoft Excel add-in program, and 4) as any deterministic optimization algorithm, it can catch the absolute lower minimum in the trapped valley.

Table 3 introduces the values of the different variables, used to generate the analytical and MOC results, to calibrate any suggested function for P in the case of the HDPE and the PVC pipes only. To limit the calculation effort, the variables that

appeared in the water hammer problem for elastic pipe, which lead to the linear change of the velocity along C^+ , are considered fixed in the present analysis as: $\alpha = 1$, $\rho = 998 \text{ kg/m}^3$, $k = 2.1\text{E}+9 \text{ Pa}$, $D = 0.05 \text{ m}$, $V_0 = 1 \text{ m/s}$, and $f = 0.02$. Anyway, the ranges of variations in α , ρ , k , and f are limited, the flowing liquid is water with nearly constant values of ρ and k , while values of α and f are around 1 and 0.02, respectively.

Total number of runs, N_i , from the different alternatives between the variable's values, shown in Table 3, is 1680. Two sets of data are used to represent the variable R , $R \leq 1$ and $R > 1$, see Table 3. For all runs, N_D is taken equal to 5000 and the output data are collected every 50-time steps with $N_j = 200$ rows of data for every run. The output data at any run i and time step j are $(D/e, J_0, J/J_0, \tau, R)_i, T_{i,j}$, and $\Delta H_{vi,j}$.

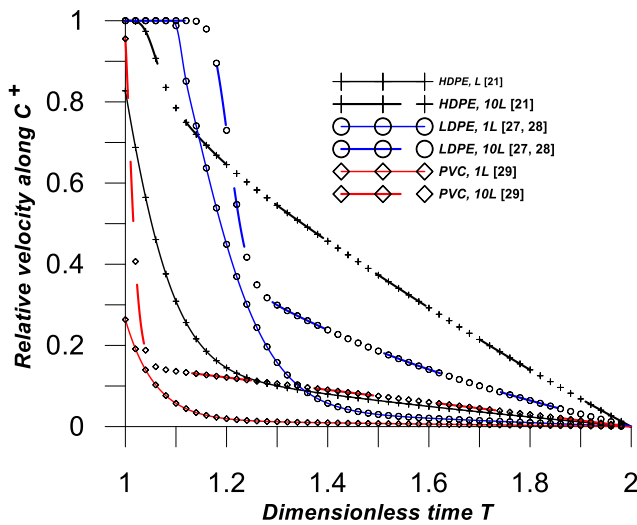


Fig. 8 Relative velocity along C^+ from the tank to the valve.

TABLE (3)
VALUES OF DIFFERENT VARIABLES USED TO CALIBRATE THE FUNCTION P

D/e	10, 14
$J_0 \times 10^{-10} \text{ Pa}^{-1}$	3, 6, 9, 12, 16
$\Sigma J/J_0$	0.01, 0.05, 0.1, 0.3, 0.5, 0.7, 1
$\tau (s)$	0.05, 0.1, 0.15, 0.2
$R (\leq 1)$	0.05, 0.1, 0.25, 0.5, 0.75, 1
$R (> 1)$	1.1, 1.3, 1.5, 1.7, 1.9, 2
N_k	1

Accurate simulation of the problem for MDPE or LDPE pipes is unavailable because it requires a huge number of the time steps and number of nodes N_D , to satisfy both the requirements of the minor retarded time at the first Kelvin element and the lengthy pipe corresponding to the dimensionless variable R .

Various suggested functions for P are examined to minimize the objective function, (21). Every suggested function is optimized several times starting from different initial values, for

the unknown decision variables, to enhance the probability of catching the most global minimum. As a rule of thumb, increasing the number of terms and associated number of decision variables improves the optimal solution, but with a diminishing rate. On the other hand, generating a function with lower number of terms and decision variables are more practical and easier in application. Therefore, variables that have a minor ability to improve the optimal solution is omitted to simplify the final form of the suggested function. The following two functions are created as:

$$P = 6.29 - 3.54(\Sigma J/J_0)^{1.89} \quad \text{for } R \leq 1 \quad (22a)$$

$$P = 5.17 - 2.6(\Sigma J/J_0)^{0.73} \quad \text{for } 1 < R \leq 2 \quad (22b)$$

Previous functions are applicable only for the HDPE and the PVC pipes. Equation (22a) is based on the values of the first set of data for R (Table 3) and is applicable only for $R \leq 1$ with a lower expected error. Whereas (22b) is based on the second set of data for $1 < R \leq 2$ which represents a longer pipe but with lesser accuracy. Each of the functions is consisting of two terms and three decision variables and mainly dependent on the degree of the viscoelasticity for the pipe. By trials, P can be considered reasonably equal to 2 for the LDPE and the MDPE pipes.

Comparison is made between the analytical and numerical results of the change in the pressure head at the valve $h_v(T)$, during the first pressure half-cycle taking the dimensionless variable R equal to one, Fig. 9. Most of the cases in Table 1 are considered and the pipe length of any case is adjusted to assure $R = 1$, as $L = 2aDR/(fV_0)$. The same curves, in Fig. 9, represent the magnitudes of the pressure head at the end of the first half cycle of the pressure, $h_v(2)$, for values of R within the range 0 to 1. An additional case for the water hammer in elastic pipe is added for sake of comparison, i.e., the upper straight line in Fig. 9. Table 4 presents the following results for every studied case with $R = 1$: 1) pipe length L , 2) $N_{Dmin} = 1 + 2L/(a \times \tau_{min})$, 3) $h_v(2)$, 4) RAMAX error for the pressure head at the valve h_v , and 5) RAMAX error for the propagated pressure head wave, Δh , along C^+ from the valve to the tank using both N_{Dmin} and 5000, respectively. Equation (22b) is reapplied with $R = 2$ for all the cases in Table 1, and the calculated RAMAX errors for both h_v and Δh_v , with $ND = 5000$, are presented in the last two columns in Table 4. Values for the different parameters of the cases in Table 1, which used to test the suggested P functions, are varied from the corresponding parameter values used to calibrate the P functions, see Table 3. That discrepancy provides a good validation for the P functions and a reliable measuring of the expected errors for any other different pipe parameters.

Table (4)
RAMAX ERROR IN h_v AND Δh FOR $R = 1$ AND 2

Plastic types	Ref.	R=1						R=2	
		(1) L (m)	(2) ND _{min}	(3) h _v (2)	(4) RAMAX h _v	(5) RAMAX Δh _{NDmin}	(6) RAMAX Δh _{ND=5000}	(7) RAMAX h _v	(8) RAMAX Δh _{ND=5000}
HDPE	[3,20]	2923	299	1.59	0.0296	0.078	0.005	0.0873	0.01
	[21]	673	159	1.57	0.0253	0.086	0.003	0.0804	0.006
	[22]	13323	1358	1.62	0.034	0.081	0.023	0.0864	0.046
	[23]	707	53	1.66	0.0304	0.099	0.001	0.1029	0.002
	[24]	5200	1606	1.69	0.0402	0.017	0.005	0.1087	0.011
MDPES	[25]	971	94054	1.15	0.149 [*] 0.0784	----- -----	0.561 0.561	0.1516 0.0783	0.644 0.644
LDPE	[26,27]	1427	105787	1.1	0.162 [*] 0.050	----- -----	0.575 0.575	0.165 0.0734	0.611 0.611
PVC	[28]	6876	627	1.87	0.0681	0.084	0.011	0.1124	0.022
	[29]	43506	5135	1.88	0.0708	0.077	0.079	0.1139	0.147

* max. error is occurred at the first time step.

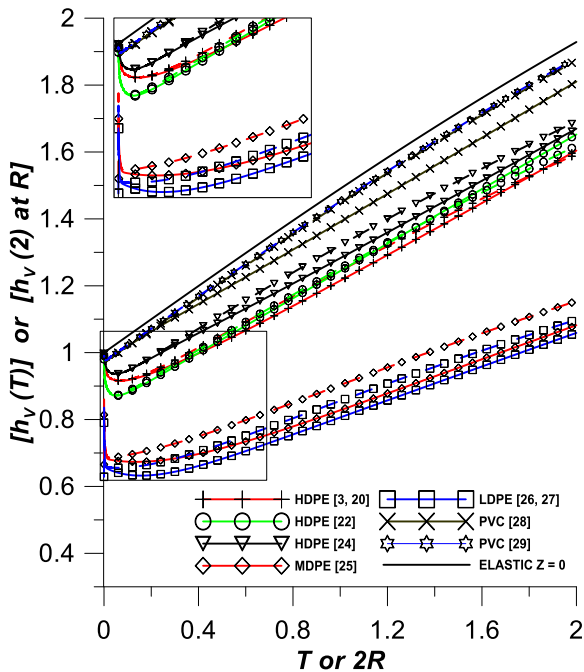


Fig. 9 h_v for the cases in Table 1. Straight and dotted lines represent analytical and MOC results, respectively.

From Fig. 9, it can be observed the degree of convergence between both the analytical and the MOC results with a relative maximum absolute error in h_v , for $R \leq 1$ and P from (22a), equal to 4.02% and 7.08% for HDPE and PVC pipes, respectively, see Table 4. In the case of MDPE or LDPE pipes, the RAMAX error is at the first time steps, but with skipping these deceptive initial steps, the second considerable maximum is less than 7.84%.

For all the studied cases, the RAMAX error in Δh decreases with increasing the number of the discretized nodes from ND_{min} to 5000. However, that error at ND_{min} is higher than the RAMAX error in h_v , with exception to the case [24], which means that the error expected from using the approximate analytical equation is always less than the error resulting from the use of the MOC with time intervals equal to $\tau_{min}/2$. Thus,

the MOC results are superior to the analytical (18b) only when using fine discretization with time step significantly less than $\tau_{min}/2$.

In the case of adopting $1 < R \leq 2$ and P from (22b), the RAMAX errors in h_v are 10.87%, 11.39%, and 7.83% for HDPE, PVC, and both MDPE and LDPE pipes, respectively, see column 8 in Table 4. The increase in the h_v error, between columns 6 and 8, is due to using the same $ND = 5000$ for the two different pipe lengths. The decrease in the pressure head, from the corresponding pressure of water hammer in case of elastic pipe, is dependent on the degree of viscoelasticity and the dimensionless coefficient R . Maximum variations in the relative pressure head between different pipe types are 0.12, 0.01, and 0.05 for HDPE, PVC, and both MDPE and LDPE, respectively. The modified P functions produce a RAMAX error which is not always located at the last time step. In general, the analytical results underestimate the pressure head at the valve.

IV. CONCLUSIONS AND RECOMMENDATIONS

Exact analytical equation, (13), is derived to determine the increase in the pressure head at the wave front caused by the sudden closure of a valve at the end of a viscoelastic pipe. This equation is used to assess the accuracy of the MOC results with different discretization schemes. An approximate analytical equation, (18 a) or (18 b), are rederived, based on Keramat and Highlight [9], to calculate the pressure head at the valve during the first half wave pressure cycle. The GRG optimization method is adopted to represent accurately the friction effect at the valve by calibrating the integration constant P , of the friction term, as a function of the different variables of the problem, (22 a) and (22 b). Several points are concluded from the present study:

- The equal relative absolute changes in the velocity and the pressure head, at the wave front during the first trip from the valve to the tank, are the same for different flow and pipe characteristics but have the same values of R and Z .

For any pipe type, as the pipe length increases and consequently Z approaches 10, the water hammer will be damped completely within the first pressure wave trip. Therefore, contrary to the elastic pipes [5], the maximum pressure head due to water hammer in viscoelastic pipes will be always involved in the first pressure wave cycle even for cross country pipes.

- For time steps equal to $\tau_{min}/2$, that is recommended as an upper limit by Covas [18], a considerable percentage of error up to 10% can be found in the MOC results. Perfect matching is observed between the proposed analytical equation and the MOC results for frictionless pipes in the case of using HDPE or PVC pipes, while insignificant error is observed in the case of MDPE pipe.
- For pipes with a minimum level of viscoelasticity as the PVC pipes, the decrease in the pressure head at the valve due to the retarded strain is overwhelming the expected increase due to the pipe backfill which leads to a decrease in the pressure head, but with a decreasing rate till zero. Hence, as the length of the pipe increases, the friction effect increases and the effect of the pipe backfill get over the viscoelasticity effect causing the pressure head to increase.
- The derived analytical equation, in association to the generated P function for adjusting the accuracy of determining the friction, can be used to obtain a fast and accurate prediction for the pressure head at the valve for all pipe types, especially for the relatively shorter pipes with $R \leq 1$. As the pipe length increases and R reaches 1, the RAMAX error increases to about 4.2% and 7.9% for the HDPE and other pipe types, respectively. These errors are comparable to the expected errors from using the MOC method with time steps equal to $\tau_{min}/2$. Thus, the MOC is preferable than the proposed analytical equation, (18 a) or (18 b), only in the case of using a high expensive number of nodes to simulate the pipe.
- The corresponding RAMAX errors for lengthy pipes which produce $1 \leq R \leq 2$ are studied. The maximum error for the pressure head at the valve increases to about 11%.

The present analytical equation is devoted to a flowing water in viscoelastic pipes, while the updated function P is concerned with only two pipe types: HDPE, and PVC. In case of MDPE and LDPE the function P can be taken as constant equal to 2. A detailed investigation of the P function is recommended as a future work to eliminate the error in the friction term.

APPENDIX A

Integration of the third term of (17) with the assumption of linear change for the velocity from the wave front to the valve along C^+ can be derived as:

$$\frac{f c(t_v)}{2gD} \int_{t_w}^{t_v} V^2 \cdot dt = \frac{f c(t_v)}{2gD} \int_{t_w}^{t_v \approx 2t_w} V_w^2 \left(2 - \frac{t}{t_w}\right)^2 \cdot dt = \frac{f c(t_v) V_w^2 t_w}{2gD \cdot 3} = \frac{f t_w V_w^2 \frac{1}{3} V_0^2 L}{2gD \cdot 3 V_0^2 L} \frac{g \Delta H_0}{a V_0} = \frac{RT v_w^2 \Delta H_0}{3} \quad (A.1)$$

APPENDIX B

Integration of the first term of (17) can be simplified as:

$$\int_{t_w}^{t_v} \frac{g}{c} \frac{dH}{dt} dt = \int_{t_w}^{t_v} \left[g \frac{d}{dt} \left(\frac{H}{c} \right) - g H \frac{d}{dt} \left(\frac{1}{c} \right) \right] dt \approx g \left(\frac{H_v |_{t_v}}{c(t_v)} - \frac{H_w |_{t_w}}{c(t_w)} \right) - \frac{g(H_w + H_v)}{2} \left(\frac{1}{c(t_v)} - \frac{1}{c(t_w)} \right) \approx g \left(\frac{H_v |_{t_v}}{c(t_v)} - \frac{*H_w |_{t_w}}{c(t_w)} \right) \quad (B.1)$$

The hydraulic head along the positive characteristic curve C^+ is considered a constant equal to the average magnitude $(H_w + H_v)/2$. As both of $c(t_w)$ and $c(t_v)$ decrease to $c(\infty)$ exponentially with time, the difference between their reciprocals diminishes and can be neglected with insignificant effect.

FUNDING STATEMENT

This research did not receive any specific grant from funding agencies in the public, commercial, or not-for-profit sectors.

DECLARATION OF CONFLICTING INTERESTS STATEMENT

The author declared that there are no potential conflicts of interest with respect to the research authorship or publication of this article.

ACKNOWLEDGEMENTS

The author wishes to thank Dr. Berge Djebedjian, Professor at Mechanical Engineering Department, Mansoura University for providing language help, precise reviewing for the derived equations and the inspiration of the research idea. Special thanks to Dr. Emad Elbeltagi, Professor at Structural Engineering Department, Mansoura University for his critical review of the work language and writing arrangement.

REFERENCES

- [1] M.S. Ghidaoui, M. Zhao, D.A. McInnis, D.H. Axworthy, "A review of water hammer theory and practice", *Appl. Mech. Rev.* vol. 58, no. 1, pp. 49-76, Jan. 2005. <https://doi.org/10.1115/1.1828050>.
- [2] H.A.A. Abdel-Gawad, B. Djebedjian, "Modeling water hammer in viscoelastic pipes using the wave characteristic method", *Appl. Math. Model.* vol. 83, pp. 322-341, 2020. <https://doi.org/https://doi.org/10.1016/j.apm.2020.01.045>.
- [3] D. Covas, I. Stoianov, J.F. Mano, H. Ramos, N. Graham, C. Maksimovic, "The dynamic effect of pipe-wall viscoelasticity in hydraulic transients. Part II - Model development, calibration and verification", *J. Hydraul. Res.*, vol. 43, pp. 56-70, 2005. <https://doi.org/10.1080/00221680509500111>.
- [4] G. Bertaglia, M. Ioriatti, A. Valiani, M. Dumbser, V. Caleffi, "Numerical methods for hydraulic transients in visco-elastic pipes", *J. Fluids Struct.*, vol. 81, pp. 230-254, 2018. <https://doi.org/10.1016/j.jfluidstruct.2018.05.004>.

- [5.] J.C.P. Liou, "Understanding line packing in frictional water hammer", J. Fluids Eng. Trans. ASME., vol. 138, no. 8, pp. 081303 1-6, Aug. 2016. <https://doi.org/10.1115/1.4033368>.
- [6.] D.J. Leslie, A.S. Tijsseling, "Travelling discontinuities in waterhammer theory: Attenuation due to friction", in: Proc. 8th BHR Gr. Int. Conf. Press. Surges (The Hague, Netherlands, April 12-14, 2000), Professional Engineering Publishing, 2000. https://www.win.tue.nl/~atijssel/pdf_files/Leslie-Tijsseling_2000.pdf.
- [7.] J. Ellis, "Pressure transients in water engineering: A guide to analysis and interpretation of behaviour", Thomas Telford Limited, 2009, p. 540.
- [8.] A. Miller, Y. Stokes, "Simple analysis of line packing, attenuation, and rarefaction phenomena in water hammer", J. Hydraul. Eng., ASCE, vol. 143, no. 10, pp. 06017017 1-7, 2017. [https://doi.org/10.1061/\(ASCE\)HY.1943-7900.0001367](https://doi.org/10.1061/(ASCE)HY.1943-7900.0001367).
- [9.] A. Keramat, A. Haghighi, "Straightforward transient-based approach for the creep function determination in viscoelastic pipes", J. Hydraul. Eng., vol. 140, pp.04014058 1-9, 2014. [https://doi.org/10.1061/\(ASCE\)HY.1943-7900.0000929](https://doi.org/10.1061/(ASCE)HY.1943-7900.0000929).
- [10.] S.E. Jons, D.J. Wood, "An exact solution of the waterhammer problem in a single pipeline with simulated line friction", ASME, PVP, vol. 140, pp. 21-26, 1988.
- [11.] J. Bohorquez, M.F. Lambert, A.R. Simpson, "Identifying head accumulation due to transient wave superposition in pipelines", J. Hydraul. Eng., ASCE, vol. 146, no. 1, pp. 04019044 1-12, 2020. [https://doi.org/10.1061/\(ASCE\)HY.1943-7900.0001631](https://doi.org/10.1061/(ASCE)HY.1943-7900.0001631).
- [12.] S.Y. Han, D. Hansen, G. Kember, "Multiple scales analysis of water hammer attenuation", Q. Appl. Math., vol. 69, pp. 677-690, Jul. 2011 <https://doi.org/10.1090/s0033-569x-2011-01258-9>.
- [13.] E. Yao, G. Kember, D. Hansen, "Analysis of water hammer attenuation in applications with varying valve closure times", J. Eng. Mech., ASCE, vol. 141, no. 1, pp. 04014107 1-9, 2015. [https://doi.org/10.1061/\(ASCE\)EM.1943-7889.0000825](https://doi.org/10.1061/(ASCE)EM.1943-7889.0000825).
- [14.] C.C. Mei, H. Jing, "Pressure and wall shear stress in blood hammer Analytical theory", Math. Biosci., vol. 280, pp.62-70, 2016. <https://doi.org/10.1016/j.mbs.2016.07.007>.
- [15.] E. Yao, G. Kember, D. Hansen, "Water hammer analysis and parameter estimation in polymer pipes with weak strain-rate feedback", J. Eng. Mech., ASCE, vol. 142, pp.1-10, 2016. [https://doi.org/10.1061/\(ASCE\)EM.1943-7889.0001104](https://doi.org/10.1061/(ASCE)EM.1943-7889.0001104).
- [16.] R.J. Sobey, Analytical solution of non-homogeneous wave equation, Coast. Eng. J., vol. 44, pp.1-23, 2002. <https://doi.org/10.1142/S057856340200041X>.
- [17.] R.J. Sobey, "Analytical solutions for unsteady pipe flow, J. Hydroinformatics", vol. 6, pp.187-207, 2004. <https://doi.org/10.2166/hydro.2004.0015>.
- [18.] D.I.C. Covas, "Inverse transient analysis for leak detection and calibration of water pipe systems modelling special dynamics effects", PhD Thesis., Imp. Coll. Sci. Technol. Med. Civ. Environ. Eng., 2003. [https://doi.org/http://www.civil.ist.utl.pt/~didia/Publications/Didia%20PhD%20Thesis%20Final%20-%20complete%20\(2003\).pdf](https://doi.org/http://www.civil.ist.utl.pt/~didia/Publications/Didia%20PhD%20Thesis%20Final%20-%20complete%20(2003).pdf).
- [19.] E. Kreyszig, H. Kreyszig, E.J. Norminton, "Advanced engineering mathematics", JOHN WILEY & SONS, INC., 2011. <http://www.wiley.com/college/kreyszig>.
- [20.] D. Covas, I. Stoianov, H. Ramos, N. Graham, C. Maksimovic, "The dynamic effect of pipe-wall viscoelasticity in hydraulic transients. Part I—experimental analysis and creep characterization", J. Hydraul. Res., vol. 42, no. 5, pp. 517-531, 2004. <https://doi.org/10.1080/00221686.2004.9641221>.
- [21.] C. Apollonio, D.I.C. Covas, G. de Marinis, A. Leopardi, H.M. Ramos, "Creep functions for transients in HDPE pipes", Urban Water J., vol. 11, no. 2, pp. 160-166, 2014. <https://doi.org/10.1080/1573062X.2012.758295>.
- [22.] J. Gong, A.C. Zecchin, M.F. Lambert, A.R. Simpson, "Determination of the creep function of viscoelastic pipelines using system resonant frequencies with hydraulic transient analysis", J. Hydraul. Eng., vol. 142, pp. 04106023 1-12, 2016. [https://doi.org/10.1061/\(ASCE\)HY.1943-7900.0001149](https://doi.org/10.1061/(ASCE)HY.1943-7900.0001149).
- [23.] S. Evangelista, A. Leopardi, R. Pignatelli, G. de Marinis, "Hydraulic transients in viscoelastic branched pipelines", J. Hydraul. Eng., vol. 141, pp. 04015016 1-9, 2015. [https://doi.org/10.1061/\(ASCE\)HY.1943-7900.0001030](https://doi.org/10.1061/(ASCE)HY.1943-7900.0001030).
- [24.] G. Pezzinga, B. Brunone, S. Meniconi, "Relevance of pipe period on kelvin-voigt viscoelastic parameters: 1D and 2D inverse transient analysis", J. Hydraul. Eng., vol. 142, pp.1-12, 2016. [https://doi.org/10.1061/\(ASCE\)HY.1943-7900.0001216](https://doi.org/10.1061/(ASCE)HY.1943-7900.0001216).
- [25.] A. Bergant, A.S. Tijsseling, J.P. Vítkovský, D.I.C. Covas, A.R. Simpson, M.F. Lambert, "Parameters affecting water-hammer wave attenuation, shape and timing - Part 1: Mathematical tools", J. Hydraul. Res., vol. 46, pp. 373-381, 2008. <https://doi.org/10.3826/jhr.2008.2848>.
- [26.] K. Urbanowicz, M. Firkowski, "Effect of creep compliance derivative in modeling water hammer in viscoelastic pipes", in: Proc. 13th Int. Conf. Press. Surges, 2018: pp. 305-324. https://doi.org/https://www.researchgate.net/publication/329759743_Effect_of_creep_compliance_derivative_in_modeling_water_hammer_in_viscoelastic_pipes.
- [27.] M. Gally, M. Gu' ney, E. Rieutord, "An investigation of pressure transients in viscoelastic pipes", J. Fluids Eng. Trans. ASME., vol. 101, pp. 495-499, 1979. <https://doi.org/https://doi.org/10.1115/1.3449017>.
- [28.] A.K. Soares, D.I.C. Covas, L.F.R. Reis, "Analysis of PVC pipe-wall viscoelasticity during water hammer", J. Hydraul. Eng., ASCE, vol. 134, pp. 1389-1394, 2008. [https://doi.org/10.1061/\(ASCE\)0733-9429\(2008\)134:9\(1389\)](https://doi.org/10.1061/(ASCE)0733-9429(2008)134:9(1389)).
- [29.] A. Bergant, Q. Hou, A. Keramat, A.S. Tijsseling, A. Gajic, M. Benisek, M. Nedeljkovic, "Experimental and numerical analysis of water hammer in a large-scale PVC pipeline apparatus", 4-th International Meeting on Cavitation and Dynamic Problems in Hydraulic Machinery and Systems, October, Belgrade, Serbia, 26-28, 2011, https://doi.org/https://www.researchgate.net/publication/241888245_Experimental_and_numerical_analysis_of_water_hammer_in_a_large-scale_PVC_pipeline_apparatus.
- [30.] A. Bergant, A.S. Tijsseling, J.P. Vítkovský, D.I.C. Covas, A.R. Simpson, M.F. Lambert, "Parameters affecting water-hammer wave attenuation, shape and timing—Part 2: Case studies", J. Hydraul. Res., vol. 46, pp. 382-391, 2008. <https://doi.org/10.3826/jhr.2008.2847>.

Title Arabic:

حل تحليلي محسن لمطرقة الماء في الأنابيب اللدنة

Abstract Arabic:

يتمثل التحدي في هذه الورقة في تحسين الحل التحليلي لمطرقة الماء أحادية البعد في خط أنابيب لدن بسبب الإغلاق المفاجئ للصمام الطرفي. تكمن أهمية الحل التحليلي في توفير معلومات التصميم الضرورية، خاصة في حالة عدم وجود برنامج حسابي للتحليل. تم اشتقاق معادلة تحليلية جديدة دقيقة لا بعدية لتحديد رأس موجة الضغط على طول رحلة موجة الضغط الأولى، وتم دمج تأثير اللدونة في سرعة الموجة. بعد ذلك، تم استخدام عملية التكامل لإعادة اشتقاق معادلة تحليلية تقريبية لرأس الضغط عند الصمام خلال نصف دورة موجة الضغط الأولى، والتي تتضمن أقصى ضغط تصميمي. تمت مقارنة أداء النتائج التحليلية مع النتائج العددية لطريقة الخصائص، تقريباً لجميع الأبحاث السابقة للمشكلة. وتم الحصول على أداء جيد للنتائج التحليلية للأنابيب غير الاحتكاكية والتي ساءت قليلاً في حاله زيادة نسبة الطاقة المهذرة نتيجة الاحتكاك المستقر في الأنابيب إلى طاقة موجة الضغط. لذلك، تم اعتماد خوارزمية تعظيم غير خطية لتحسين ثابت التكامل لمصطلح الاحتكاك، مما عزز دقة النتائج التحليلية.